PTP1B promotes focal complex maturation, lamellar persistence and directional migration

Juan E. Burdisso, Ángela González and Carlos O. Arregui*

Instituto de Investigaciones Biotecnológicas, Universidad de San Martín/CONICET, 1650 San Martín, Buenos Aires, Argentina

*Author for correspondence (carregui@iib.unsam.edu.ar)

Accepted 21 January 2013
Journal of Cell Science 126, 1820–1831

doi: 10.1242/jcs.118828

Summary

Previous findings established that ER-bound PTP1B targets peripheral cell–matrix adhesions and positively regulates cell adhesion to fibronectin. Here we show that PTP1B enhances focal complex lifetime at the lamellipodium base, delaying their turnover and facilitating α-actinin incorporation. We demonstrate the presence of catalytic PTP1BD181A–α-actinin complexes at focal complexes. Kymograph analysis revealed that PTP1B contributes to lamellar protrusion persistence and directional cell migration. Pull-down and FRET analysis also showed that PTP1B is required for efficient integrin-dependent downregulation of RhoA and upregulation of Rac1 during spreading. A substrate trap strategy revealed that FAK/Src recruitment and Src activity are essential for the generation of PTP1B substrates in adhesions. PTP1B targets the negative regulatory site of Src (phosphotyrosine 529), paxillin and p130Cas at peripheral cell–matrix adhesions. We postulate that PTP1B modulates more than one pathway required for focal complex maturation and membrane protrusion, including α-actinin-mediated cytoskeletal anchorage, integrin-dependent activation of the FAK/Src signaling pathway, and RhoA and Rac1 GTPase activity. By doing so, PTP1B contributes to coordinated adhesion turnover, lamellar stability and directional cell migration.

Key words: PTP1B, Adhesion, Migration, Src, FAK

Introduction

Cell migration requires a regulated adhesion assembly–disassembly cycle. Advance of the protruding cell edge occurs concomitantly with the appearance of nascent adhesions within the lamellipodium (Choi et al., 2008). As the leading edge moves forward, nascent adhesions grow and turn into focal complexes, which at the lamellipodium base may turnover or grow further and mature into elongated focal, and fibrillar adhesions (Vicente-Manzanares et al., 2009; Scales and Parsons, 2011).

PTP1B is a non-receptor protein tyrosine phosphatase bound to the cytosolic face of the endoplasmic reticulum (ER) through a hydrophobic C-terminal tail (Frangioni et al., 1992). PTP1B is present in complexes of β1- and β3-integrin (Arregui et al., 1998; Arias-Salgado et al., 2005), and interacts with the adaptor protein p130Cas, which in part localizes at focal adhesions (Harte et al., 1996; Liu et al., 1996). As the catalytic domain of PTP1B faces the cytosol, it has the potential for substrate dephosphorylation throughout the extensive branching network occupied by the ER. Indeed, PTP1B has been shown to dephosphorylate plasma membrane receptors (Ahmad et al., 1995; Elchebly et al., 1999; Buckley et al., 2002; Haj et al., 2002), protein adaptors (Garton et al., 1996), and cytosolic tyrosine kinases such as Src (Arregui et al., 1998; Bjorge et al., 2000). Identification of most PTP1B substrates was made possible by the generation of effective substrate trapping mutants, such as PTP1BDA, in which the invariant catalytic aspartic acid 181 is replaced by alanine (Flint et al., 1997). This mutation increases substantially the steady-state population of PTP1BDA–substrate complexes, allowing their direct visualization by optical techniques. Interactions between ER-bound PTP1BDA and endocytosed EGFR and PDGFR have been detected as puncta by Förster resonance energy transfer (FRET) (Haj et al., 2002), and by cryo-immunoelectron microscopy (Eden et al., 2010). PTP1BDA interactions with targets localized at integrin and cadherin adhesion complexes, as well as with EphA3/ephrin-mediated cell–cell contacts, seem to occur at the cell surface (Arregui et al., 1998; Balsamo et al., 1998; Hernández et al., 2006; Hernández et al., 2010; Nievergall et al., 2010; Haj et al., 2012).

We previously reported that ER-bound GFP–PTP1BDA accumulates in puncta over peripheral cell–matrix adhesions (Hernández et al., 2006). However, the identity of substrates to which this mutant trap binds in adhesions, and the functional consequences of PTP1B activity, remained elusive. By time-lapse analysis we have now directly demonstrated that focal complexes in cell protrusions extend their lifetimes when contacted by active ER-bound PTP1B. We demonstrate the presence of catalytic PTP1BDA/α-actinin in focal complexes and show that α-actinin is essentially absent from focal complexes of PTP1B null cells, suggesting an inefficient coupling to actin cytoskeleton. Kymograph analysis revealed that PTP1B promotes the persistence of leading edge protrusions and the directionality of cell migration. We also show that PTP1B modulate integrin-dependent regulation of RhoA and Rac1 GTPases, and present compelling evidence suggesting that in addition to α-actinin, Src, paxillin and p130Cas are PTP1B substrates targeted at adhesions.

Results

ER-bound PTP1B regulates adhesion lifetimes during lamellar protrusion

Mechanisms underlying turnover or maturation of focal complexes at the lamellipodium base are poorly understood (Geiger et al., 2009; Vicente-Manzanares et al., 2009; Scales and

Parsons, 2011). Based on previous antecedents showing that PTP1B is positioned over peripheral paxillin adhesions by tubular extensions of the ER (Hernández et al., 2006), and that peripheral adhesions targeted by ER tubules subsequently grew in size (Zhang et al., 2010), we hypothesized that PTP1B on the surface of the ER could regulate adhesion lifetime during cell protrusion. We tested this hypothesis in immortalized fibroblasts derived from PTP1B-deficient mouse (KO cells) (Haj et al., 2002) transfected with mRFP-paxillin to label adhesions, and either GFP-PTP1B wild type (WT) or GFP-PTP1B (CS), a catalytically inactive mutant with the essential cysteine 215 substituted by serine (Guan and Dixon, 1991; Flint et al., 1997). WT and CS expression did not significantly affect the spatial organization and dynamics of the ER [(Arregui et al., 1998) and results not shown]. Time-lapse analysis revealed that ER tubules containing WT and CS targeted paxillin adhesions assembled at or near the leading edge (Fig. 1A; supplementary material Fig. S1; Movies 1, 2). Target events occurred mainly during the growing phase of adhesions (97%, $n=34$ adhesions, 8 cells), as judged by the increase of mRFP–paxillin fluorescence intensity over time. In addition, adhesions targeted by WT lasted longer than those targeted by CS (compare Fig. 1A and Fig. 1B). Quantification of adhesion lifetime, measured as the time span from the first appearance of a resolvable mRFP–paxillin cluster until complete disassembly, revealed that in KO cells expressing CS, targeted and non targeted adhesions have similar lifetimes, ranging from 1–12 minutes, with a median of 4 minutes (Fig. 1C, CS_T and CS_{NT}). These results were similar to those of non targeted paxillin clusters in KO cells expressing WT (Fig. 1C, WT_{NT}). However, adhesions targeted with WT increased dramatically their lifetimes, ranging from 11 to 36 minutes, with a median of 20 minutes (Fig. 1C, WT_T). We also analyzed the lifetime of peripheral mRFP–paxillin adhesions in KO cells and KO cells stably reconstituted with PTP1BWT (WT cells) (Haj et al., 2002). We found a wide range of adhesion lifetimes, with a median of 24 minutes for WT cells and 18 minutes for KO cells. Interestingly, the number of adhesions with lifetime ≤7 minutes was 2.5-fold higher in KO cells compared to WT cells (Fig. 1D). However, the number of adhesions with longer lifetimes was similar or higher in WT cells implicating that PTP1B contributes to stabilize focal complexes assembled during lamellar protrusion.

PTP1B regulates paxillin turnover and promotes incorporation of α-actinin in focal complexes

To further investigate the function of PTP1B in adhesions we determined the paxillin assembly/disassembly rate constants in WT and KO cells transfected with mRFP-paxillin, using methods

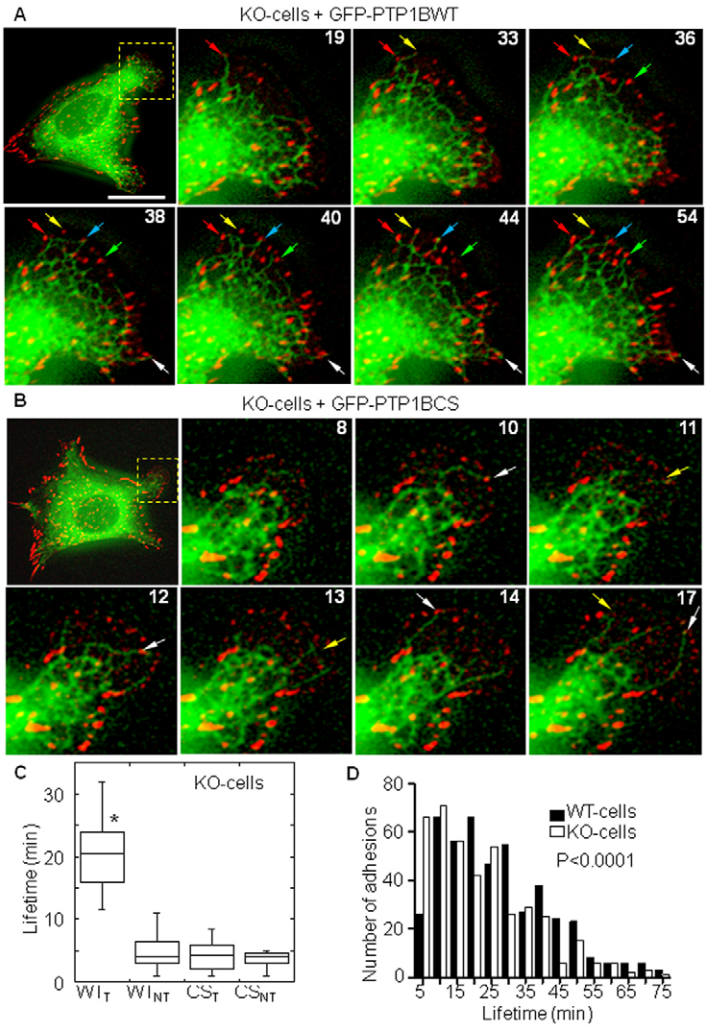

Fig. 1. ER-bound PTP1B regulates adhesion lifetimes during lamellar protrusions. KO cells expressing mRFP–paxillin and either (**A**) GFP–PTP1BWT (WT) or (**B**) GFP–PTP1BCS (CS) were analyzed by time-lapse microscopy. A protruding lamella, marked by a dashed yellow box in the first frame, was magnified (4×) to illustrate targeting events. A targeting event is defined as an event in which the tip of a single ER tubule is found juxtaposed to one mRFP–paxillin cluster. Numbers in each frame indicate minutes elapsed since the beginning of the experiment. Arrows point to a single targeting event in the first and subsequent frames in which they were observed. (A) Adhesions targeted with WT (color arrows) persisted and grew in size. (B) Four different targeting events of CS occurred at 10, 12, 14 and 17 minutes (white arrows). The first three targeted foci disappeared at 11, 13, and 17 minutes, respectively (yellow arrows). (**C**) Quantification of adhesion lifetimes targeted (WT_T, CS_T) and non-targeted (WT_{NT}, CS_{NT}). Each box in the plot encloses 50% of the data and the line marks the median value. Lines extending from the top and bottom of each box mark the minimum and maximum values within the data set. *Significant difference when compared to the other conditions ($P<0.0001$, one-way ANOVA followed by a Tukey's HSD *post-hoc* test). (**D**) Frequency distribution plot (numbers on the abscissa mark the center of the bin size; 5 minutes) of lifetime adhesions in WT and KO cells. Data were analyzed by a Wilcoxon–Mann–Whitney non-parametric test. Note that short-lived adhesions (≤7 minutes) in KO cells duplicated those in WT cells. Scale bar: 25 μm.

previously described (Franco et al., 2004; Webb et al., 2004). In both cell lines paxillin assembly and disassembly rate constants correlated inversely with adhesion lifetimes (Fig. 2A). Assembly rate constants did not differ significantly between WT and KO cells (WT, 0.50±0.04 versus KO, 0.66±0.05). However, disassembly rates were significantly higher in KO cells compared to WT cells (WT, 0.44±0.03 versus KO, 0.70±0.06; Fig. 2A). To test if this result could be due to more abundant short-lived adhesions in KO cells, we sorted a similar number of short-lived adhesions (≤10 minutes, $n=28$ adhesions/5 cells) for each cell line. Although these pools displayed similar lifetimes (WT mean: 7.1 minutes versus KO mean: 6.5 minutes), paxillin disassembly rates were significantly higher in KO cells compared to WT cells (WT, 0.77±0.07 versus KO, 1.17±0.10), while assembly rate constants did not differ (WT, 0.85±0.08 versus KO, 1.04±0.10). These results suggest that the prevalence of short-lived paxillin adhesions in KO cells is most likely a consequence of their higher disassembly rates. Adhesions with longer lifetimes (>15 minutes), did not show significant differences in paxillin disassembly rates between WT and KO cells (WT, 0.27 versus KO, 0.24, $P=0.4$), suggesting that a major impact of PTP1B activity is on the newly born population.

As the leading edge advances, some adhesions grow and elongate centripetally, often accompanied by the incorporation of α-actinin (Laukaitis et al., 2001). Alpha actinin mediates integrin-actin cytoskeleton linkages in a process that is negatively regulated by tyrosine phosphorylation of α-actinin (Izaguirre et al., 2001; von Wichert et al., 2003). Since PTP1B dephosphorylates α-actinin (Zhang et al., 2006), we predicted a failure in α-actinin incorporation to focal complexes in KO cells. WT- and KO cells were co-transfected with α-actinin-GFP and mRFP-paxillin and analyzed by time-lapse microscopy. During protrusion, α-actinin–GFP strongly labeled the lamellipodium, which contained small clusters of mRFP–paxillin (Fig. 2B,C). As the lamellipodium moved forward, paxillin clusters remained stationary and grew in size. About 98.7±3.7% of paxillin clusters in WT cells incorporated α-actinin in a polar fashion and grew centripetally compared to only 22.2±7% in KO cells (Fig. 2B,D,F; supplementary material Movies 3, 4). When lamellae retracted, paxillin foci in WT and KO cells incorporated α-actinin in similar manner, suggesting that PTP1B contributes to anchor new adhesions to the actin cytoskeleton during protrusions. To directly visualize catalytic PTP1B–α-actinin complexes in adhesions of intact WT cells we performed bimolecular fluorescence complementation (BiFC) analysis (Hu et al., 2002). Catalytic PTP1B–substrate complexes can be visualized only when their steady state concentration is significantly increased by using substrate trapping mutants of PTP1B, such as the PTP1B D181A (DA) (Haj et al., 2002; Boute et al., 2003; Monteleone et al., 2012). Indeed, co-expression of YN-PTP1BWT/α-actinin-YC (YN, amino acids 1–154; YC, amino acids 155–238 of EYFP) did not reveal a detectable BiFC signal (supplementary material Fig. S2). In contrast, co-expression of YN-PTP1BDA/α-actinin-YC exhibited bright BiFC

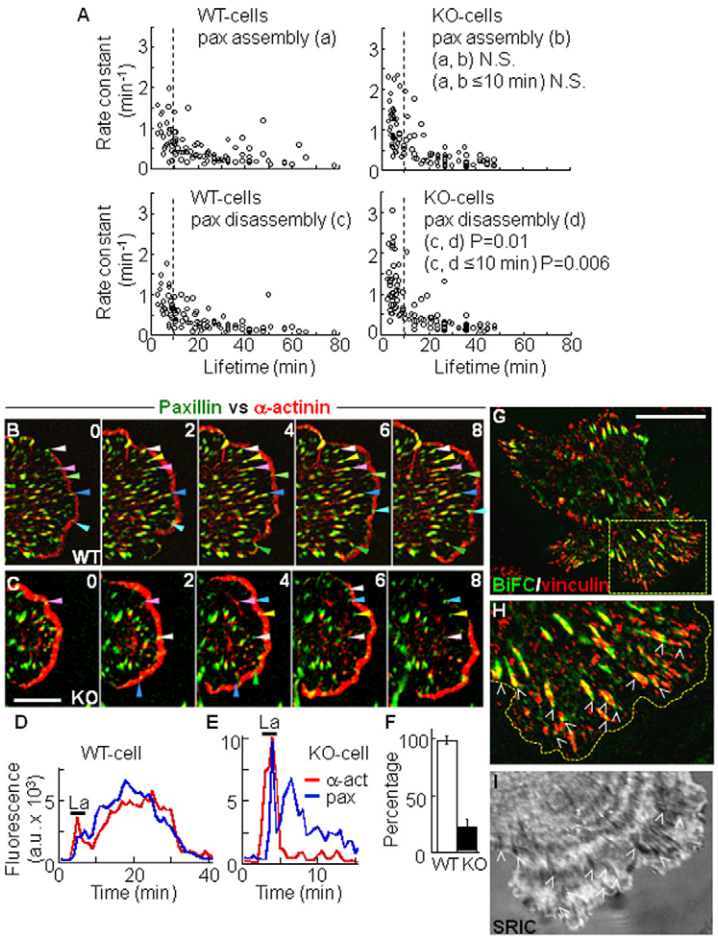

Fig. 2. PTP1B regulates paxillin turnover and incorporation of α-actinin in cell protrusions. (**A**) mRFP–paxillin assembly and disassembly rate constants are inversely correlated with adhesion lifetimes in both WT and KO cells. Global disassembly rates in KO cells were higher than in WT cells ($P=0.01$), a difference that is magnified in a subset of short-lived adhesions (≤10 minutes, marked by dashed lines; WT, 28 adhesions; KO, 43 adhesions; $P=0.006$). Data were analyzed by the Wilcoxon–Mann–Whitney non-parametric test. N.S.: $P>0.05$. (**B**) In WT cells, most mRFP–paxillin adhesions (in green) at the lamellipodium base (arrowheads) incorporated α-actinin–GFP (in red). (**C**) In KO cells, mRFP–paxillin quickly turned over without incorporation of α-actinin–GFP. (**D**,**E**) Plot profiles of mRFP–paxillin- and α-actinin–GFP-integrated fluorescence intensities over time, in representative WT and KO cells. The first fluorescence peak is within the lamellipodium (La). Note that in the WT cell both plot profiles overlap spatially and temporally (D), but those in the KO cell only overlap within the lamellipodium (E). (**F**) Percentages of mRFP–paxillin foci that incorporated α-actinin during the time-lapse assay. Bars represent means ± s.e.m. of 8–9 cells and 36–47 adhesions per condition (Student's *t*-test, $P<0.0001$). Scale bar: 12 μm. (**G**,**H**) WT cell co-transfected with YN-PTP1BDA/α-actinin-YC BiFC pairs and immunolabeled for vinculin (in red). H is an enlarged view of the boxed region in G. (**I**) A surface reflection interference contrast image. A representative polarized cell depicting a protruding lamella (right lower corner) is shown. Note that BiFC is strong and punctate in peripheral adhesions, although the overlapping area varies (white open arrowheads). Scale bars: 25 μm (G), magnifications in H and I are at 200% of the original image.

signal in peripheral clusters containing the YN-PTP1BDA construct (supplementary material Fig. S2). This distribution is prevented by pre-incubation with pervanadate, which inactivates the active site of the enzyme. The estimated expression levels of YN-PTP1BDA (and α-actinin-YC, not shown) associated to this BiFC signal was ~1.5–2-fold of the endogenous proteins. Each BiFC pair transfected individually showed the expected subcellular distribution and did not display detectable fluorescence in the BiFC channel (supplementary material Fig. S2) (Monteleone et al., 2012). We analyzed the presence of the BiFC signal in adhesions by immunofluorescence detection of vinculin and by surface reflection interference contrast (SRIC) imaging. The BiFC signal significantly overlapped with vinculin and (low reflection) dark peripheral adhesions in protruding regions of the cell (Fig. 2G–I).

PTP1B promotes lamellar protrusion persistence and directional cell migration

To determine if unstable focal complexes in KO-cell protrusions affected lamellar dynamics, we performed kymograph analysis of the leading edge in WT and KO cells transfected with α-actinin–GFP. Visual inspection of kymographs showed persistent protrusions in WT cells and fast protrusion/retraction cycles in KO cells (Fig. 3A,B; supplementary material Movies 5, 6). Quantifications revealed an approximately fivefold higher frequency of protrusion/retraction switching in KO cells compared with WT cells (WT cells, 1.36±0.24/hour versus KO cells, 7.20±0.70/hour; Fig. 3C). In addition, KO cells exhibited an approximately threefold reduction in protrusion persistence times compared to WT cells (WT cells, mean 16.82±1.46 minutes versus KO cells, mean 5.22±0.49 minutes), while retraction persistence times was marginally affected (WT cells, 4.63±0.44 minutes versus KO cells, 3.86±0.20 minutes; Fig. 3D). Protrusion speed increased approximately threefold in KO cells (WT cells, 40.8±2.60 μm/hour versus KO cells, 125±8.00 μm/hour), and retraction speed approximately twofold (WT cells, 48.70±4.10 μm/hour, KO cells, 115.20±6.90 μm/hour), compared to WT cells (Fig. 3E). These results suggest that PTP1B contributes to the steady protrusion of the leading edge.

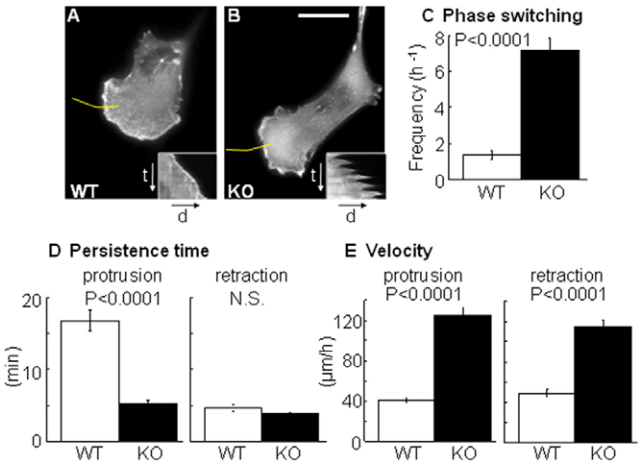

Fig. 3. PTP1B regulates lamellar dynamics. WT and KO cells expressing α-actinin–GFP were analyzed by kymography. (**A**,**B**) Individual frames at t0 and kymographs (insets) of representative cells. The fluorescence intensity along line scans (1-pixel wide) drawn normal to the border of the protruding lamella (yellow lines) was recorded every 30 seconds for 50 minutes. Note the smooth advance of the leading edge in the WT cell compared to the serrated, discontinuous advance of the leading edge in the KO cell. 't' and 'd' indicate time and space dimensions, respectively. (**C**) Plot showing higher frequencies of protrusion/retraction cycles in KO cells compared to WT cells, $n=10$ cells, $P<0.0001$. (**D**) Persistence time of protrusion phases was markedly reduced (approximately threefold) in KO cells compared to WT cells ($P<0.0001$) whereas persistence time did not differ. WT=10 cells, 53 kymographs; KO=11 cells, 106 kymographs. (**E**) Velocities of protrusion and retraction phases were calculated from the slopes. Cell protrusions: $n=68$ WT, $n=69$ KO; retractions: $n=22$ WT, $n=50$ KO. $P<0.0001$. Data were analyzed by the Wilcoxon–Mann–Whitney non-parametric test. N.S. indicates a $P>0.05$. Scale bar: 35 μm.

We also analyzed the directionality, speed and migratory patterns of WT and KO cells under two-dimensional isotropic conditions. Under these conditions, single cells follow an almost straight path over short time intervals, yet exhibiting Brownian-like motion over long time intervals, which can be mathematically characterized as a persistent random walk (Gail and Boone, 1970; Dunn, 1983; Othmer et al., 1988). We collected time-lapse phase contrast videos of cells moving on fibronectin during a 10 hour period and reconstructed their trajectories. A representative set of cell trajectories revealed that WT cells exhibit longer and more directional paths than KO cells (Fig. 4A). WT cells developed a large lamellar extension at the front edge while KO cells produced transient lamellar extensions in multiple directions (Fig. 4B; supplementary material Movies 7, 8). Long trailing tails were frequent in KO cells and rare in WT cells. We quantified migration directionality as the ratio between the shortest linear distance from the starting point of a time-lapse recording to the end point (D), and the total distance (T) traversed by the cell (Gu et al., 1999). This D/T ratio equals to one in the case of ballistic motion. D/T ratios were significantly lower in KO cells compared to WT cells (WT cells, 0.64±0.02 versus KO cells, 0.42±0.04), suggesting a decrease of directionality (Fig. 4C). KO cells also had slower migration speed (WT cells, 12.8±0.18 μm/hour versus KO cells, 9.6±0.13 μm/hour; Fig. 4C). These results were confirmed by fitting the mean square displacements (MSD) of cell paths over time to the random walk equation. The MSD was calculated and plotted against time using the Cell Motility software (Martens et al., 2006). In pure random movement MSD variations would appear as a straight line passing through the origin while in a ballistic motion it would fit to an exponential curve. The averaged MSD of >29 cells plotted against time showed higher displacements and a more curved line in WT cells compared to KO cells (Fig. 4C). To extract speed (S) and persistence (P) parameters, MSD data were fitted to the random walk model using a Nelder–Mead simplex non-linear regression algorithm (Martens et al., 2006). S and P were significantly reduced in KO cells compared to WT cells (S, WT cells, 15.1±1.9 μm/hour versus KO cells, 10.4±0.30 μm/hour; P, WT cells, 6.0±0.91 hours versus KO cells, 3.3±0.66 hours). Since KO cells displayed persistent trailing tails and unstable leading edges, we predicted an alteration of the migration pattern. Thus, we examined arrays of color-coded advance and pause phases, arranged as they occur within the time-lapse series. Arrays revealed a seemingly higher prevalence of pauses in KO cells compared to WT cells (Fig. 4D; WT cells, 11.35±1.40%, $n=28$ versus KO cells, 21.16±1.73%, $n=31$, $P<0.0001$).

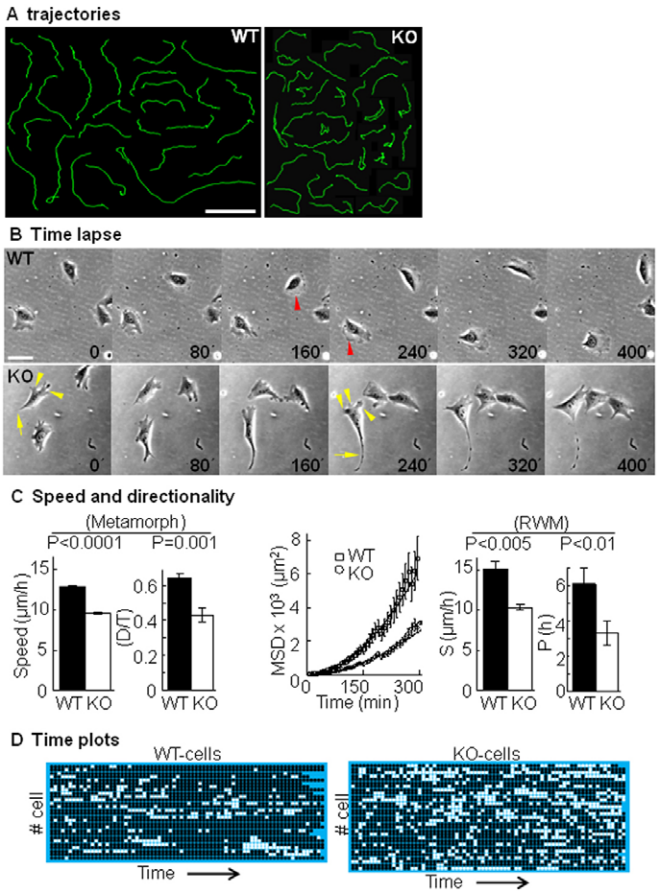

Fig. 4. PTP1B promotes persistent migration. WT and KO cells were analyzed by time-lapse phase-contrast microscopy. (**A**) Randomly selected individual tracks of WT and KO cells were copied and combined into single panels to avoid empty spaces. Scale bar: 100 μm. (**B**) Phase-contrast image sequences of representative WT and KO cells. WT cells form broad and persistent lamellar extensions in the direction of migration (red arrowheads) whereas KO cells form narrow and low persistence lamellar extensions in several directions (yellow arrowheads), and frequently have long trailing tails (yellow arrows). Numbers indicate time in minutes. Scale bar: 50 μm. (**C**) Quantification of migration speed and directionality. Averaged speed, calculated with Metamorph software, was significantly reduced in KO cells ($P<0.0001$). Migration directionality was determined by calculating the D/T ratio, and by fitting the MSD to the persistent random walk model (RWM) equation. Note that D/T in WT cells is significantly higher than that in KO cells ($P=0.001$). The MSD over time was used to extract values of speed (S) and persistence time (P). Data were analyzed by the Wilcoxon–Mann–Whitney non-parametric test. Bars represent the means ± s.e.m. of 29–32 cells. (**D**) Time plots of the migratory pattern of WT and KO cells. Advance and pause phases of each time-lapse series were color-coded (black square=advance, white square=pause; each square=time interval of 8 minutes) and arranged in a horizontal row as they occurred. Intervals with a net advance lower to 1.3 μm were considered as pauses.

Integrin-dependent regulation of RhoA and Rac1 is impaired in PTP1B null cells

Stimulation of integrins and growth factor receptors regulate RhoA and Rac1 GTPases (Bar-Sagi and Hall, 2000; Schwartz and Shattil, 2000; Burridge and Wennerberg, 2004). In turn, GTPase activity coordinates the dynamics of the actin cytoskeleton and cell–matrix adhesions during cell migration (Vicente-Manzanares et al., 2009; Scales and Parsons, 2011). Serum starved WT cells plated on fibronectin for 15 minutes showed a well-defined F-actin-rich lamellipodium and few actin stress fibers. In contrast, KO cells did not produce a lamellipodium; instead they exhibited spiky margins and prominent actin stress fibers (Fig. 5A). These observations suggest impaired Rac1 and RhoA activities in KO cells. We quantified the active GTP-bound RhoA and Rac1 by pull-down assays. RhoA–GTP levels in WT cells were downregulated after plating on fibronectin, reaching ~20% of the value of cells in suspension by 30 minutes post-plating (Fig. 5B). Downregulation of RhoA–GTP levels did not occur in KO cells. We also quantified the Rac1–GTP levels. Soon after seeding on fibronectin (10 minutes), WT cells increased Rac1–GTP levels which almost doubled those of cells in suspension (Fig. 5B). In contrast, KO cells showed no response. We confirmed these results in individual cells by FRET analysis. WT and KO cells were transfected with single-chain FRET pRaichu biosensors, which monitor RhoA and Rac1 activities at the cell membrane (Itoh et al., 2002; Yoshizaki et al., 2003). GTPase activity, expressed as a FRET/CFP ratio for each pixel, was visualized using the intensity modulation display mode, which associates color hue with ratio values and the intensity of each hue with the source image brightness (Tsien and Harootunian, 1990). Red and blue colors in images represent the spatial distribution of high and low GTPase activity, respectively. In WT cells plated on fibronectin RhoA activity was downregulated while Rac1 activity was induced. The opposite was observed in KO cells (Fig. 5C). RhoA activity in KO cells and Rac1 activity in WT cells were maximal at the cell margin and decrease gradually towards the cell center. To quantify these observations we calculated the FRET/CFP ratios along line scans traced normal to the cell border. Adhesion to polylysine, as a non specific substrate, showed a similar increase of RhoA and Rac1 activity in WT cells and KO cells. However, adhesion to fibronectin showed higher RhoA in KO cells, and Rac1 in WT cells (Fig. 5C). These results suggest that PTP1B promotes integrin-dependent Rac1 activation and RhoA repression.

PTP1B targets substrata of the Src/FAK signaling pathway in adhesions

Our previous time-lapse studies demonstrated that GFP–PTP1BDA form fluorescent puncta over the distal pole of peripheral mRFP–paxillin adhesions in a time-dependent manner (Hernández et al., 2006). BiFC and FRET studies also have observed PTP1BDA/substrate complexes as fluorescent clusters (Haj et al., 2002; Anderie et al., 2007; Nievergall et al., 2010; Monteleone et al., 2012). In the present study the BiFC signal for YN-PTP1BDA/α-actinin-YC were also observed as puncta in more peripheral adhesions. These puncta were absent in cells pre-incubated with pervanadate (a general inhibitor of PTPs) or transfected with the wild-type enzyme. Thus, we assumed that GFP–PTP1BDA fluorescent puncta associated with peripheral adhesions reflect the accumulation of enzyme/substrate complexes, and predicted that removal of those substrates from adhesion sites should prevent the formation of puncta. We screened cell lines knockout for proteins that fulfilled three conditions: (1) that were previously identified as PTP1B substrates; (2) that were detected in cell-matrix adhesion sites; and (3) that were involved in integrin-dependent signaling pathways regulating RhoA and Rac1 GTPases. These included

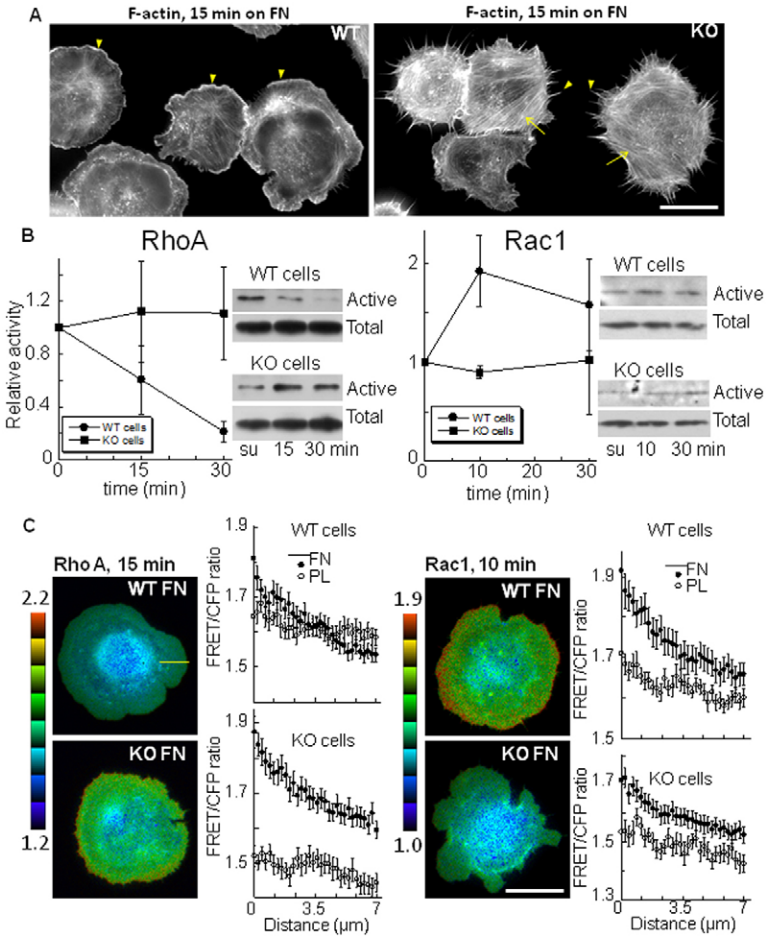

Fig. 5. PTP1B modulates fibronectin-dependent regulation of RhoA and Rac1 activity. (**A**) Serum-starved WT and KO cells were seeded on polylysine + fibronectin-coated coverslips for 15 minutes and labeled with TRITC–phalloidin. WT cells showed a strong F-actin staining at lamellipodia (yellow arrowheads). KO cells showed F-actin in stress fibers (yellow arrows) and peripheral spikes (yellow arrowheads). Scale bar: 25 μm. (**B**) Results of pull-down assays to quantify GTP-bound RhoA and Rac1 in cells in suspension or plated on fibronectin-coated dishes. Values of active GTPases were normalized to total GTPases. Plots show the means ± s.e.m. of three independent experiments and are expressed relative to the suspension value. Representative blots are also shown. (**C**) Spatiotemporal distribution of RhoA and Rac1 activities, by FRET. Cells were seeded on polylysine and polylysine + fibronectin (FN) for the indicated times to determine the FRET signal. Representative cells on FN are shown. Graphs show the quantification of the FRET/CFP ratio values along line scans drawn from the cell margin, as shown in the WT FN RhoA image (n=15–20 cells per condition). Scale bar: 25 μm.

cells knockout for the adaptor proteins p130Cas and paxillin, and for the protein tyrosine kinases FAK and Src. As control, we examined a cell line derived from a littermate wild-type mouse. On average, ~62.0±2.4% of vinculin peripheral adhesions in control cells displayed associated GFP–PTP1BDA puncta (Fig. 6A,H). This percentage was reduced in cells null for Src (44.9±3.2%), paxillin (46.3±2.4%) and p130Cas (37.8±2.7%; Fig. 7B–D,H). However, the most dramatic effect was observed in SYF cells, which lack the expression of Src, Fyn and Yes members of the Src family (1.8±0.5%) and in FAK KO cells (2.7±0.9%) (Fig. 6E,F,H). A strong effect was also observed in wild-type cells transfected with FRNK, a FAK-related non kinase protein which displaces FAK from adhesions (supplementary material Fig. S3) (Richardson et al., 1997). GFP–PTP1BDA did not develop puncta in peripheral adhesions containing FRNK (Fig. 6G,H). These results suggest that FAK expression and localization at peripheral adhesions are both essential for the generation of PTP1B substrates.

Downstream of integrin and growth factor stimulation, FAK is autophosphorylated at −397, providing a binding site for Src family kinases (Schaller et al., 1994). Reconstitution of FAK KO cells with GFP–FAK induced formation of mRFP–PTP1BDA puncta at adhesions (52.4±5%) while reconstitution with FAK Y397F did not (0.3±0.2%; Fig. 7B,I). These results suggest that Src recruitment to adhesions by FAK Tyr397 is essential for trapping PTP1BDA.

Reconstitution of SYF cells with Src-HA rescued the formation of puncta at adhesions (73.6±3.8%; Fig. 7C,I), and a similar result was observed for Fyn-HA and Yes-HA (supplementary material Fig. S4). These results suggest compensatory roles among Src family members. SYF cells reconstituted with a kinase-deficient (KD) Src mutant (Src K297R), which as expected, was unable to phosphorylate FAK Tyr925 (supplementary material Fig. S5) (Brunton et al., 2005), showed a marginal effect (14.7±3.4%) to induce the formation of GFP–PTP1BDA puncta associated with adhesions (Fig. 7D,I). In contrast, reconstitution of SYF cells with Src-Y529F, a constitutive active mutant that preferentially localizes in cell–matrix adhesions and increase the phosphotyrosine content of several substrata (Kaplan et al., 1994; Cary et al., 2002), induced the accumulation of large puncta (69.5±4.1%; Fig. 7E,I). These results demonstrate that localization and activity of Src at cell–matrix adhesions are required for recruitment of GFP–PTP1BDA puncta. Reconstitution of SYF cells with the double mutant Src KD/Y529F, which localizes to adhesions but lacks both the catalytic activity and the PTP1B target site pY529 (Bjorge et al., 2000; Monteleone et al., 2012), was unable to induce the formation of puncta (1.5±0.6%; Fig. 7F,I). Thus, the residual fraction of puncta induced by Src KD expression is likely due to the binding of the pTyr529 by PTP1BDA, in particular at high expression levels of Src KD (supplementary material Fig. S5). Consistent with this notion, no residual puncta of GFP–PTP1BDA were observed in SYF cells at high expression levels of the double mutant KD/Y529F (supplementary material Fig. S6).

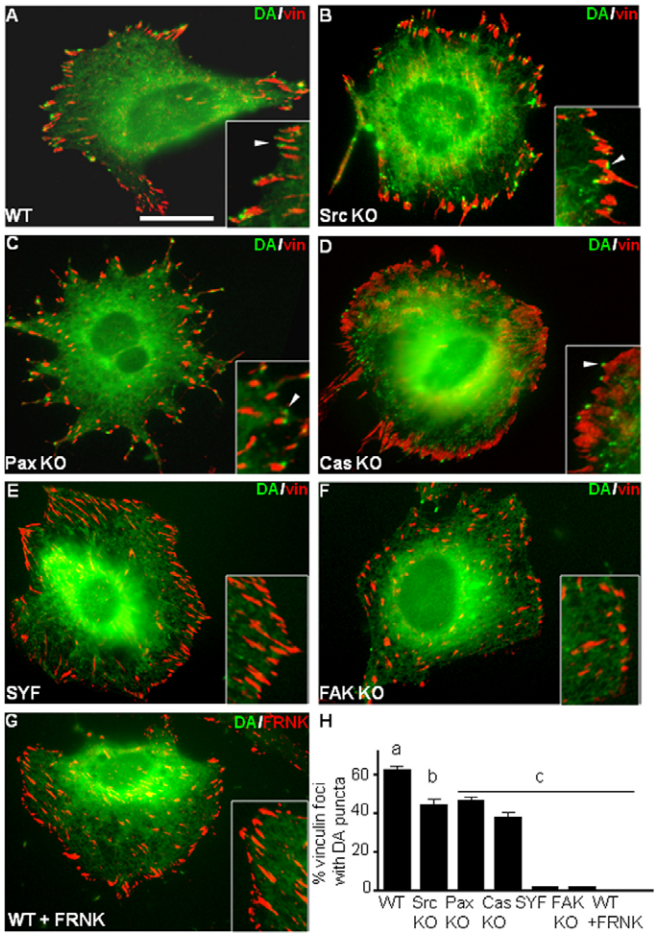

Fig. 6. PTP1B targets Src/FAK, paxillin and p130Cas in cell–matrix adhesions. (**A**) WT control fibroblast cell, (**B**) Src null cell, (**C**) Paxillin null cell, (**D**) p130Cas null cell, (**E**) SYF cell, (**F**) FAK null cell. Cell lines were transfected with GFP-PTP1BDA. (**G**) WT control co-transfected with GFP-PTP1BDA and c-myc FRNK. Cells were fixed and processed for immunofluorescence microscopy to detect vinculin (A–F) or c-myc (G). Immune complexes were revealed with Alexa-Fluor-568-conjugated secondary antibodies. Insets are 2× magnifications of part of each cell. GFP–PTP1BDA puncta associated with peripheral adhesions are indicated by white arrowheads. (**H**) Quantification of the percentage of peripheral adhesions containing GFP–PTP1BDA puncta. Puncta were significantly reduced in Src, Pax, and Cas knockout cells, and essentially absent in SYF, FAK KO cells and WT cells + FRNK. Statistical significance was determined using one-way ANOVA followed by the Dunnett's multiple comparison *post-hoc* test, using the WT cell line as the control ($^{a,b}P=0.0002$; $^{a,c}P<0.0001$). Scale bar: 25 μm.

We also examined the effect of reconstituting SYF cells with Src Y418F, which cannot autophosphorylate but could still be activated by integrin stimulation (Kaplan et al., 1995; Cary et al., 2002; Roskoski, 2005). Src Y418F induced a maximal effect, as did Src wild type and Src Y529F (70±2.4%; Fig. 7G,I). However, the double mutant Src Y418F/Y529F induced a reduced effect (49.6±5.3%) compared to Src wild type and the individual mutants (Fig. 7H,I). Src Y418F (not shown) and Src Y418F/Y529F phosphorylate FAK-Tyr925 at similar levels as control Src (compare supplementary material Fig. S6 and Fig. S5). Thus, basal or partly activated Src may be sufficient to trap PTP1BDA at peripheral vinculin adhesions. The magnitude of reduction of puncta formation (~20%) by Y418F/Y529F compared to Src Y418F is similar to that between Src KD and Src KD/Y529F suggesting that PTP1BDA is capable of recognizing the phosphorylated Src Tyr529 in peripheral adhesions.

Discussion

PTP1B regulates focal complex dynamics

PTP1B anchored to the ER, and with the catalytic domain facing the cytosol, has the potential for substrate dephosphorylation throughout the extensive branching network occupied by the ER. Here we demonstrated that paxillin adhesions targeted with ER tubules bearing active PTP1B extended by approximately fivefold their lifetimes compared to those not targeted, or targeted with ER tubules bearing inactive PTP1B. Consistently, we also found that short-lived adhesions (≤10 minutes) were significantly more abundant in KO cells compared to WT cells. We propose that during lamellar protrusion, ER-bound PTP1B targets newly formed adhesions and as a consequence bias their fate towards maturation. During retraction phases adhesions grew in size independently of PTP1B expression, suggesting that this bias is overrode when additional mechanisms, e.g. contractile forces, come into play. Consistent with this notion, lack of PTP1B strongly affected protrusion persistence times but not retraction times. Our results provide mechanistic insights to previous findings suggesting a positive regulation of cell matrix–adhesion and spreading by PTP1B in many cell types (Arregui et al., 1998; Cheng et al., 2001; Pathre et al., 2001; Arias-Salgado et al., 2005; Liang et al., 2005; Fuentes and Arregui, 2009).

The increased paxillin disassembly kinetics observed in KO cells may contribute to shorten the lifetime of focal complexes. This view agrees with results showing that adhesion lifetime correlates positively with adhesion strength and inversely with paxillin disassembly (Gupton and Waterman-Storer, 2006). Adhesion strength and inhibition of paxillin adhesion disassembly at the lamellipodium base were also positively correlated with the incorporation of α-actinin and zyxin (Laukaitis et al., 2001; von Wichert et al., 2003; Zaidel-Bar et al., 2003; Yoshigi et al., 2005; Choi et al., 2008; Hirata et al., 2008). We previously demonstrated that zyxin incorporation in focal complexes was significantly impaired in KO cells (Hernández et al., 2006). Here we show that in WT cells most focal complexes at the lamellipodium base incorporated α-actinin–GFP and grow centripetally, while in KO cells these processes were impaired. Our BiFC analysis demonstrate the presence of catalytic PTP1B/α-actinin complexes in adhesions, strongly suggesting that PTP1B dephosphorylates α-actinin and promotes focal complex maturation. During lamellar retractions, adhesions incorporate α-actinin similarly regardless of PTP1B expression, suggesting that PTP1B did not play a major role during this phase. Whether other PTPs, e.g. SHP-1 and SHP-2 (von Wichert et al., 2003; Lin et al., 2004) may dephosphorylate α-actinin during retractions remains to be determined.

PTP1B modulates integrin-dependent regulation of RhoA and Rac1

We show that fibronectin stimulated the downregulation of RhoA activity in WT- but not in KO cells. In contrast, Rac1 activity was upregulated in WT cells but not in KO cells. WT cells response to fibronectin was consistent with previous studies (Ren et al., 1999; Arthur et al., 2000; del Pozo et al., 2000; Danen et al., 2002; Lim et al., 2008). Spatial information provided by FRET analysis showed maximal Rac1 and RhoA activity at the cell periphery, as

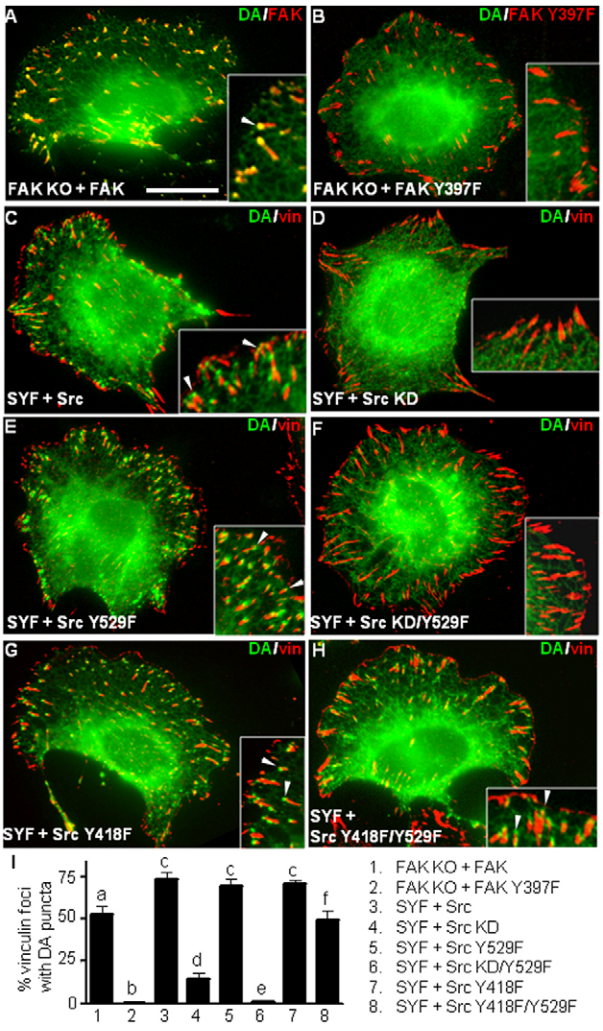

Fig. 7. FAK/Src activity is required to trap PTP1BDA in adhesions. (**A**,**B**) FAK KO cells were transfected with mRFP-PTP1BDA and reconstituted with (A) GFP–FAK or (B) GFP–FAK-Y397F. Colors were inverted for better visualization. (C–H) SYF cells co-transfected with GFP-PTP1BDA and Src (**C**), Src KD (**D**), Src Y529F (**E**), Src KD/Y529F (**F**), Src Y418F (**G**) or Src Y418F/Y529F (**H**). In all these cells vinculin was detected by immunofluorescence. GFP–PTP1BDA puncta associated with peripheral vinculin adhesions (in red) are indicated by white arrowheads in the insets (2× magnification). (**I**) Plot shows percentages of peripheral adhesions containing GFP–PTP1B puncta. Statistical significance was determined using one-way ANOVA followed by the Tukey's HSD *post-hoc* test ($^{a,b}P<0.0001$; $^{c,d;\ c,e}P<0.0001$; $^{c,f}P=0.001$). Scale bar: 25 µm.

described in other cell types (Nakamura et al., 2005; Pertz, 2010). The high RhoA and low Rac1 activities in KO cells could explain the lack of a lamellipodium and the development of actin stress fibers shown by phalloidin staining. Unbalanced contractile forces generated in the lamella could explain the low protrusion persistence during migration.

PTP1B stabilizes lamellar protrusions and promotes directional migration

The increased focal complex turnover in KO cells may be causally related to the lower persistence of the leading edge and the loss of migration directionality. Consistent with this notion impairment of cell–matrix adhesion in CHO.K1 cells reduced the stability of protrusions and migration directionality (Harms et al., 2005). In a reciprocal manner, forced integrin clustering in fibroblasts promoted focal adhesion development and lamellar persistence (Cavalcanti-Adam et al., 2007). Our results suggest that PTP1B is seemingly implicated in the regulation of processes occurring at different time scales, like adhesion turnover, lamellar dynamics and directional migration. Mechanistically, PTP1B may facilitate integrin/cytoskeleton coupling by dephosphorylation of α-actinin. PTP1B may also promote integrin-dependent signaling regulating RhoA and Rac1 GTPases and the actin cytoskeleton, such as the Src/FAK signaling pathway. Strikingly, several morphological and motility alterations shown by KO cells resemble those reported in fibroblasts deficient in FAK expression (Tilghman et al., 2005).

PTP1B substrates in adhesions

Our BiFC results strongly suggest that PTP1B dephosphorylate α-actinin at cell–matrix adhesions. This event may facilitate cytoskeletal coupling and focal complex maturation, as previously reported (Laukaitis et al., 2001; Rajfur et al., 2002; von Wichert et al., 2003; Choi et al., 2008). A previous model proposed that phosphorylated α-actinin could form a complex with Src and compete for the binding of Src to FAK (Zhang et al., 2006). In accordance with this model, α-actinin dephosphorylation by PTP1B would facilitate the assembly of Src/FAK complexes and likely the phosphorylation of downstream substrates. We showed that the substrate trap mutant GFP–PTP1BDA formed puncta associated to peripheral adhesions in control cells, but not in FAK KO cells, in cells expressing FRNK, and in SYF cells. In addition, reconstitution with catalytically inactive mutants were unable to recover the formation of puncta. These results clearly indicate that FAK and Src activity are essential for generating tyrosine phosphorylated substrates of PTP1B in adhesions. We recently have shown that PTP1B targets the negative regulatory site of Src, Tyr529, at the plasma membrane/substrate interface (Monteleone et al., 2012). This result suggests PTP1B could activate Src and FAK, and initiate phosphorylation of downstream targets, including α-actinin, paxillin and p130Cas. Paxillin and p130Cas are phosphorylated by FAK and Src, and their phosphorylated species localize in focal adhesions (Bellis et al., 1995; Schaller and Parsons, 1995; Schaller et al., 1999; Sakai et al., 1997; Tachibana et al., 1997; Fonseca et al., 2004). We observed a modest, but significant decrease of GFP–PTP1BDA puncta in paxillin and p130Cas KO cells, suggesting a direct dephosphorylation of paxillin and p130Cas by PTP1B in adhesions. Our results agree with previous biochemical data proposing that paxillin and p130Cas are direct PTP1B substrates (Liu et al., 1996; Takino et al., 2003; Dubé et al., 2004). Since phosphorylation of paxillin and p130Cas are required for adhesion turnover (Webb et al., 2004), PTP1B may negatively modulate this process.

Collectively, our results suggest a complex interplay of PTP1B effects. The effect on Src activation could initiate downstream protein phosphorylation in adhesions, mounting an early integrin-dependent signaling response channeled to GTPases. PTP1B could also dephosphorylate specific Src/FAK substrates, modulating the timing of complex events, like cell–matrix turnover, lamellar dynamics, and directional migration. A

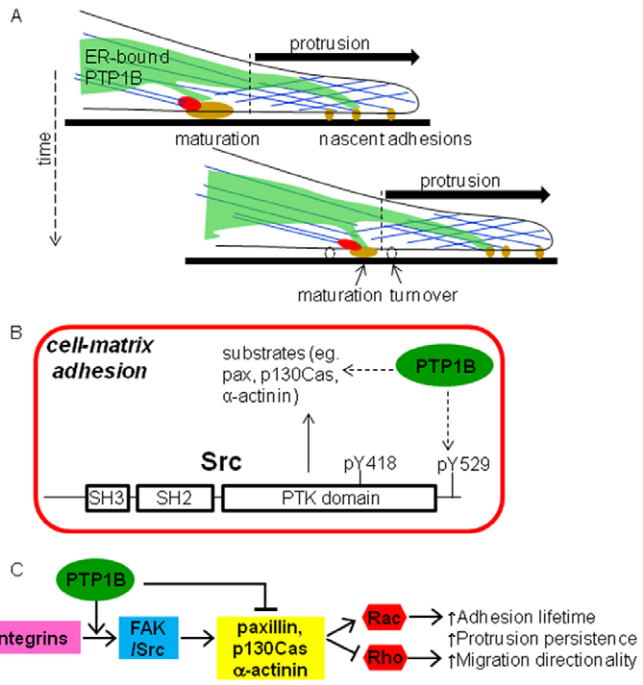

Fig. 8. Schematic representation of PTP1B functions in adhesion and cell migration. (**A**) Adhesions near the leading edge (brown circles) are targeted by ER-bound PTP1B (green), extending their lifetimes, incorporating α-actinin (red oval), and coupling to actin filaments (in blue). (**B**) Within cell adhesion complexes, PTP1B targets Src and also modulates the phosphorylation level of downstream substrates. (**C**) PTP1B is required for integrin-dependent FAK/Src signaling that regulates Rho GTPases.

scenario representing the interpretation of our data are shown schematically (Fig. 8).

Materials and Methods

Cell lines, materials and treatments

The following cell lines were kindly provided by colleagues: KO and WT cells (B. Neel, University Health Network, Toronto, Ontario; Haj et al., 2002), Src knockout and wild type fibroblasts (P. Soriano, Fred Hutchinson Research Center, Seattle, WA; Klinghoffer et al., 1999), paxillin wild-type and knockout cells (S. M. Thomas, Harvard Medical School, Boston; Hagel et al., 2002), wild-type and p130Cas knockout cells (H. Honda, Hiroshima University, Japan; Honda et al., 1998). SYF and FAK knockout cell lines were purchased from ATCC (Manassas, VA). All cell lines were cultured in high glucose DMEM containing L-glutamine plus 10% fetal bovine serum and antibiotics (Invitrogen, Carlsbad, CA). Polylysine and fibronectin were from Sigma-Aldrich (St. Louis, MO). For microscopy, cells were on coverslips (Marienfeld GmbH & Co, Lauda-Königshofen, Germany) or custom-made coverslip-bottom dishes. When indicated, cells were preincubated for 30 minutes with 0.1 mM sodium pervanadate before processing, as described (Hernández et al., 2010).

Antibodies and other labeling reagents

TRITC-conjugated phalloidin, and monoclonal anti-vinculin (clone hVIN-1), anti-HA (clone HA-7), and anti-c-myc (clone 9E10) were from Sigma-Aldrich (St Louis, MO, USA). Polyclonal antibodies against GFP, FAK-pY397, FAK-pY925, Src-pY529, Src-pY418, and Alexa-Fluor-488- and 568-conjugated antibodies were from Invitrogen. HRP-conjugated antibodies were from Jackson ImmunoResearch (West Grove, PA).

DNA constructs and transfections

GFP-PTP1B, D181A and C215S, and mRFP-paxillin were previously described (Arregui et al., 1998; Hernández et al., 2006). The following plasmids were provided by colleagues: pRaichu-Rac1 (1026×) and pRaichu-RhoA (1237×) (M. Matsuda, Osaka University, Osaka, Japan), chicken GFP-FAK and c-myc-FRNK (J. T. Parsons, University of Virginia, Charlottesville, VA), α-actinin-GFP (C. A. Otey, University of North Carolina at Chapel Hill, Chapel Hill), chicken c-Src Y416F, mouse Fyn and Yes (J. Cooper, Fred Hutchinson Cancer Research Center, Seattle, WA), mouse Src (S. Shattil, University of California at San Diego, San Diego). Chicken c-Src Y416 was subcloned into *Bam*HI/*Hin*dIII sites of pcDNA3.1/zeo. Mouse Src, and Fyn were subcloned into *Xho*I/*Eco*RI sites of phCMV3 (Genlantis), and Yes into *Kpn*I/*Xma*I sites. This produces Src, Fyn and Yes with an HA epitope at the C-terminus. GFP-FAK Y397F and mutants, Src Y529F and Src Y418F/Y529F were constructed using the QuikChange site-directed mutagenesis kit (Stratagene, La Jolla, CA). Src KD (K297R) and Src KD/Y529F were generated by recombinant PCR. Preparation of YN-PTP1B WT/DA constructs for BiFC was previously described (Monteleone et al., 2012). Alpha actinin-YC was made by replacing GFP in α-actinin–GFP with YC (amino acid 155–239) obtained by PCR, using *Age*I/*Xba*I restriction sites. The DNA sequence of all constructs were verified by sequencing. Transient transfections were performed using Lipofectamine 2000 (Invitrogen), as described (Hernández et al., 2006).

Pull-down assays

RhoA and Rac1 activities were performed using pull-down assay kits (Cytoskeleton, Inc., Denver, CO). About 350 µg of protein (0.5 mg/ml) of cells in suspension or plated at 50–60% confluence on fibronectin-coated tissue culture dishes were used to isolate GTP-bound RhoA and Rac1 using 50 µg Rhotekin-RBD beads, and 20 µg PAK-PBD beads, respectively. Total RhoA and Rac1 proteins (from 10% of cell lysate) and the isolated active forms were detected in Western blots using the Super Signal West Femto Substrate kit (Thermo Scientific). For stripping, blots were incubated (30 minutes, 55℃) with TBS containing 5% 2-mercaptoethanol and 2% SDS, blocked and re-probed. Integrated optical densities of bands in scanned films were determined using ImageJ (Wayne Rasband, NIH, Bethesda, MD, USA). Active RhoA and Rac1 proteins were normalized to total GTPase.

Fluorescence microscopy

Cells attached on fibronectin-coated (10 µg/ml) coverslips were fixed with 4% paraformaldehyde (20 minutes), permeabilized with 0.5% Triton X-100 (5 minutes), and blocked with 5% BSA (60 minutes), all diluted in PBS (137 mM NaCl, 2.7 mM KCl, 10 mM Na_2HPO_4, 1.8 mM KH_2PO_4, pH 7.4). Primary and secondary antibodies were diluted in PBS/BSA and incubated in a humid chamber (60 minutes). Cells were mounted in Vectashield (Vector Laboratories, Burlingame, CA) and imaged using a Nikon TE 2000-U inverted microscope (Melville, NY) equipped with a 60×/1.4 NA objective, and an Orca-AG cooled CCD camera (Hamamatsu Photonics, Hamamatsu, Japan). For time-lapse experiments, cells were kept at 37℃ in Phenol-Red-free DMEM with high glucose, supplemented with 4 mM L-glutamine and 25 mM Hepes buffer, 10% fetal bovine serum, antibiotics and 0.5 U/ml oxyfluor (Oxyrase, Inc., Mansfield, OH). Culture medium was overlaid with mineral oil to prevent evaporation. EGFP and mRFP were detected using Nikon B-2E/C and G-2E/C filter sets. The excitation light was attenuated using neutral density filters and shuttered using a SmartShutter and a Lambda 10-B controller (Sutter Instrument, Novato, CA). All peripherals were controlled with Metamorph 6.1 software (Molecular Devices, Downingtown, PA). Image stacks were built using ImageJ. For display purposes images were processed for unsharp masking.

Cell migration and kymographs

WT and KO cells (10,000 cells) were seeded in 24-well tissue-culture plates coated with fibronectin and blocked with BSA. After overnight incubation, cell movements were monitored under phase contrast using a 10× objective every 8 minutes during 10 hours. Light was attenuated by ND4 filters and shuttered between acquisitions. Cells that divided or made contacts with others were not analyzed. To reconstruct cell trajectories, positions of cell nuclei were determined using the track object function of Metamorph. Velocities and persistence of migratory directionality (D/T) were extracted from recorded data. 'D' refers to the linear distance from the starting point to the end point of a time-lapse recording and 'T' refers to the total distance traversed by the cell. A list of 'x' and 'y' pixel coordinates for each cell was fed into the Cell Motility Suite software (Martens et al., 2006) to calculate the MSD over time and extract the values of speed (S) and persistence time (P) by fitting the MSD to the persistent random walk model (RWM) equation (Dunn, 1983; Othmer et al., 1988).

For kymographs, cells were transfected with α-actinin-GFP and imaged every 30 seconds during 50 minutes, using 2×2 binning. Excitation light was attenuated by ND4 filters. We used ImageJ to draw three lines (1-pixel-wide, 0.22 µm) per cell in the direction of lamellar protrusion. Leading edge protrusion and retraction rates, frequencies of switching between phases, and time of protrusion or retraction persistence were calculated from kymographs using the kymograph plugin for ImageJ (J. Rietdorf, FMI Basel, and A. Seitz, EMBL Heidelberg).

BiFC and FRET

Two α-actinin constructs were made, one fused to YN (amino acid 1–154) and other fused to YC (155–239), both EYFP fragments were located at the C-terminus of α-actinin. The correspondent PTP1B BiFC pairs were previously described

(Monteleone et al., 2012). Only the pair α-actinin-YC/YN-PTP1B DA gave a strong positive BiFC signal and were used in the present paper. BiFC was analyzed with an excitation filter of 500/20 nm, an emission filter of 535/30 nm and a 86002v2bs dicroic mirror (Chroma Technology, Brattleboro, VT). In cells detecting BiFC and immunolabeled with red fluorescents the following Nikon filter sets were used: for BiFC, excitation 480/30 nm, emission 535/40 nm, 505 (LP) dicroic mirror; for Alexa Fluor 568 nm, excitation 540/25 nm, emission 620/60 nm, 565 (LP) dicroic mirror. To visualize cells by SRIC, a cube (Nikon) with a green excitation filter, a UV dicroic mirror and without barrier filter was set in place in the epifilter rotating turret.

Spatiotemporal activities of RhoA and Rac1 in WT and KO cells were determined by FRET analysis using pRaichu-Rac1 (1026×) and pRaichu-RhoA (1294×) probes (Itoh et al., 2002; Nakamura et al., 2005). Transfected cells were starved 4 hours before plating on coverslips coated with 150 µg polylysine or polylysine plus 10 µg/ml fibronectin, and blocked with 1 mg/ml BSA. Incident light was attenuated using ND8 filters. Filters used for dual-emission ratio imaging (CFP excitation 430/25, CFP emission 470/30; YFP emission 535/30) were placed in filter wheels and combined with the dual dichroic mirror 86002v2bs (Chroma). CFP and YFP (FRET) images were acquired using 2×2 binning and exposure times ranging 0.5–1 seconds. After shade correction and background subtraction, FRET/CFP ratio images were generated with Metamorph and used to represent changes in the FRET efficiency by intensity modulated display (IMD). For quantification, pixel values for FRET and CFP along three equidistant line scans (3-pixels wide) perpendicular to the cell border were obtained, FRET/CFP ratios were calculated and averaged per cell.

Additional quantitative procedures

ER targeting events (defined in Fig. 1 legend) on paxillin adhesion lifetimes were determined in KO cells co-transfected with mRFP-paxillin and either GFP-PTP1BWT or GFP-PTP1BCS. Cells seeded on fibronectin and grown in complete DMEM were imaged every 30 seconds using 2×2 binning. The contrast of image stacks was improved by unsharp masking using ImageJ. Adhesion lifetimes were determined measuring the time elapsed between the first and last frame in which each adhesion appeared. About 50 adhesions of 6–8 cells were analyzed.

To determine adhesion lifetimes and paxillin kinetics of assembly and disassembly WT and KO cells were transfected with GFP- or mRFP-tagged paxillin and 24 hours post-transfection were resuspended and seeded at ~30% confluence on coverslip-bottom dishes coated with fibronectin. After 16 hours cells were analyzed using time-lapse acquired images every 0.5, 1 and 3 minutes. Different time intervals allowed a better sampling of short- and long-lived adhesions. Fluorescence intensities of individual adhesions from background-subtracted images were measured over time using Metamorph as previously described (Webb et al., 2004). For rate constant measurements, periods of assembly (increasing fluorescence intensity) and disassembly (decreasing fluorescence intensity) of adhesions were plotted over time. Semi-logarithmic plots of fluorescence intensities as a function of time were generated using the formulas, $\mathrm{Ln}([I]/[I0])$ for assembly and $\mathrm{Ln}([I0]/[I])$ for disassembly, where $I0$ is the initial fluorescence intensity and I is the fluorescence intensity at various time points. The slopes of linear regression trend lines fitted to the semi-logarithmic plots were then calculated to determine apparent rate constants of assembly and disassembly. At least 95 individual adhesions in 20 cells were analyzed per cell line.

To determine α-actinin–GFP incorporation in mRFP–paxillin clusters cells were imaged every 0.5 and 1 minute. After building the image stacks, plots of fluorescence intensity over time were obtained for paxillin clusters using ImageJ. Incorporation of α-actinin–GFP was considered positive when the signal intensity is at least twice higher than the background and overlaps with that of the mRFP–paxillin. Eight or nine cells and 36–47 adhesions were analyzed per condition.

To quantify the percentage of peripheral vinculin adhesions with GFP–PTP1BDA puncta we generated a mask image containing puncta with fluorescence intensity at least twice the average fluorescence intensity of the ER in a peripheral flat region of the cell, and merged it with the image showing vinculin. More than 20 cells from four independent experiments (average 26 peripheral adhesions per cell) were analyzed.

Acknowledgements

We thank Drs B. Neel, P. Soriano, S. M. Thomas, H. Honda for sharing cell lines, and M. Matsuda, J.T. Parsons, C.A. Otey, J. Cooper, S. Shattil for providing DNA constructs.

Author contributions

J.E.B. and A.G. performed the experiments; J.E.B., A.G. and C.O.A. designed the experiments and analyzed the data; C.O.A. wrote the paper.

Funding

This work was supported by Consejo Nacional de Investigaciones Científicas y Técnicas [PhD fellowship to J.E.B. and Research membership to C.O.A.]; and Agencia Nacional de Promoción Científica y Tecnológica [PhD fellowship to A.G. and grant numbers 31939 and 1363 to C.O.A.]

Supplementary material available online at
http://jcs.biologists.org/lookup/suppl/doi:10.1242/jcs.118828/-/DC1

References

Anderie, I., Schulz, I. and Schmid, A. (2007). Direct interaction between ER membrane-bound PTP1B and its plasma membrane-anchored targets. *Cell. Signal.* **19**, 582-592.

Ahmad, F., Li, P. M., Meyerovitch, J. and Goldstein, B. J. (1995). Osmotic loading of neutralizing antibodies demonstrates a role for protein-tyrosine phosphatase 1B in negative regulation of the insulin action pathway. *J. Biol. Chem.* **270**, 20503-20508.

Arias-Salgado, E. G., Haj, F., Dubois, C., Moran, B., Kasirer-Friede, A., Furie, B. C., Furie, B., Neel, B. G. and Shattil, S. J. (2005). PTP-1B is an essential positive regulator of platelet integrin signaling. *J. Cell Biol.* **170**, 837-845.

Arregui, C. O., Balsamo, J. and Lilien, J. (1998). Impaired integrin-mediated adhesion and signaling in fibroblasts expressing a dominant-negative mutant PTP1B. *J. Cell Biol.* **143**, 861-873.

Arthur, W. T., Petch, L. A. and Burridge, K. (2000). Integrin engagement suppresses RhoA activity via a c-Src-dependent mechanism. *Curr. Biol.* **10**, 719-722.

Balsamo, J., Arregui, C., Leung, T. and Lilien, J. (1998). The nonreceptor protein tyrosine phosphatase PTP1B binds to the cytoplasmic domain of N-cadherin and regulates the cadherin-actin linkage. *J. Cell Biol.* **143**, 523-532.

Bar-Sagi, D. and Hall, A. (2000). Ras and Rho GTPases: a family reunion. *Cell* **103**, 227-238.

Bellis, S. L., Miller, J. T. and Turner, C. E. (1995). Characterization of tyrosine phosphorylation of paxillin in vitro by focal adhesion kinase. *J. Biol. Chem.* **270**, 17437-17441.

Bjorge, J. D., Pang, A. and Fujita, D. J. (2000). Identification of protein-tyrosine phosphatase 1B as the major tyrosine phosphatase activity capable of dephosphorylating and activating c-Src in several human breast cancer cell lines. *J. Biol. Chem.* **275**, 41439-41446.

Boute, N., Boubekeur, S., Lacasa, D. and Issad, T. (2003). Dynamics of the interaction between the insulin receptor and protein tyrosine-phosphatase 1B in living cells. *EMBO Rep.* **4**, 313-319.

Brunton, V. G., Avizienyte, E., Fincham, V. J., Serrels, B., Metcalf, C. A., 3rd, Sawyer, T. K. and Frame, M. C. (2005). Identification of Src-specific phosphorylation site on focal adhesion kinase: dissection of the role of Src SH2 and catalytic functions and their consequences for tumor cell behavior. *Cancer Res.* **65**, 1335-1342.

Buckley, D. A., Cheng, A., Kiely, P. A., Tremblay, M. L. and O'Connor, R. (2002). Regulation of insulin-like growth factor type I (IGF-I) receptor kinase activity by protein tyrosine phosphatase 1B (PTP-1B) and enhanced IGF-I-mediated suppression of apoptosis and motility in PTP-1B-deficient fibroblasts. *Mol. Cell. Biol.* **22**, 1998-2010.

Burridge, K. and Wennerberg, K. (2004). Rho and Rac take center stage. *Cell* **116**, 167-179.

Cary, L. A., Klinghoffer, R. A., Sachsenmaier, C. and Cooper, J. A. (2002). SRC catalytic but not scaffolding function is needed for integrin-regulated tyrosine phosphorylation, cell migration, and cell spreading. *Mol. Cell. Biol.* **22**, 2427-2440.

Cavalcanti-Adam, E. A., Volberg, T., Micoulet, A., Kessler, H., Geiger, B. and Spatz, J. P. (2007). Cell spreading and focal adhesion dynamics are regulated by spacing of integrin ligands. *Biophys. J.* **92**, 2964-2974.

Cheng, A., Bal, G. S., Kennedy, B. P. and Tremblay, M. L. (2001). Attenuation of adhesion-dependent signaling and cell spreading in transformed fibroblasts lacking protein tyrosine phosphatase-1B. *J. Biol. Chem.* **276**, 25848-25855.

Choi, C. K., Vicente-Manzanares, M., Zareno, J., Whitmore, L. A., Mogilner, A. and Horwitz, A. R. (2008). Actin and alpha-actinin orchestrate the assembly and maturation of nascent adhesions in a myosin II motor-independent manner. *Nat. Cell Biol.* **10**, 1039-1050.

Danen, E. H., Sonneveld, P., Brakebusch, C., Fassler, R. and Sonnenberg, A. (2002). The fibronectin-binding integrins alpha5beta1 and alphavbeta3 differentially modulate RhoA-GTP loading, organization of cell matrix adhesions, and fibronectin fibrillogenesis. *J. Cell Biol.* **159**, 1071-1086.

del Pozo, M. A., Price, L. S., Alderson, N. B., Ren, X. D. and Schwartz, M. A. (2000). Adhesion to the extracellular matrix regulates the coupling of the small GTPase Rac to its effector PAK. *EMBO J.* **19**, 2008-2014.

Dubé, N., Cheng, A. and Tremblay, M. L. (2004). The role of protein tyrosine phosphatase 1B in Ras signaling. *Proc. Natl. Acad. Sci. USA* **101**, 1834-1839.

Dunn, G. A. (1983). Characterising a kinesis response: time averaged measures of cell speed and directional persistence. *Agents Actions Suppl.* **12**, 14-33.

Eden, E. R., White, I. J., Tsapara, A. and Futter, C. E. (2010). Membrane contacts between endosomes and ER provide sites for PTP1B-epidermal growth factor receptor interaction. *Nat. Cell Biol.* **12**, 267-272.

Elchebly, M., Payette, P., Michaliszyn, E., Cromlish, W., Collins, S., Loy, A. L., Normandin, D., Cheng, A., Himms-Hagen, J., Chan, C. C. et al. (1999). Increased insulin sensitivity and obesity resistance in mice lacking the protein tyrosine phosphatase-1B gene. *Science* **283**, 1544-1548.

Flint, A. J., Tiganis, T., Barford, D. and Tonks, N. K. (1997). Development of "substrate-trapping" mutants to identify physiological substrates of protein tyrosine phosphatases. *Proc. Natl. Acad. Sci. USA* **94**, 1680-1685.

Fonseca, P. M., Shin, N. Y., Brábek, J., Ryzhova, L., Wu, J. and Hanks, S. K. (2004). Regulation and localization of CAS substrate domain tyrosine phosphorylation. *Cell. Signal.* **16**, 621-629.

Franco, S. J., Rodgers, M. A., Perrin, B. J., Han, J., Bennin, D. A., Critchley, D. R. and Huttenlocher, A. (2004). Calpain-mediated proteolysis of talin regulates adhesion dynamics. *Nat. Cell Biol.* **6**, 977-983.

Frangioni, J. V., Beahm, P. H., Shifrin, V., Jost, C. A. and Neel, B. G. (1992). The nontransmembrane tyrosine phosphatase PTP-1B localizes to the endoplasmic reticulum via its 35 amino acid C-terminal sequence. *Cell* **68**, 545-560.

Fuentes, F. and Arregui, C. O. (2009). Microtubule and cell contact dependency of ER-bound PTP1B localization in growth cones. *Mol. Biol. Cell* **20**, 1878-1889.

Gail, M. H. and Boone, C. W. (1970). The locomotion of mouse fibroblasts in tissue culture. *Biophys. J.* **10**, 980-993.

Garton, A. J., Flint, A. J. and Tonks, N. K. (1996). Identification of p130(cas) as a substrate for the cytosolic protein tyrosine phosphatase PTP-PEST. *Mol. Cell. Biol.* **16**, 6408-6418.

Geiger, B., Spatz, J. P. and Bershadsky, A. D. (2009). Environmental sensing through focal adhesions. *Nat. Rev. Mol. Cell Biol.* **10**, 21-33.

Gu, J., Tamura, M., Pankov, R., Danen, E. H., Takino, T., Matsumoto, K. and Yamada, K. M. (1999). Shc and FAK differentially regulate cell motility and directionality modulated by PTEN. *J. Cell Biol.* **146**, 389-403.

Guan, K. L. and Dixon, J. E. (1991). Evidence for protein-tyrosine-phosphatase catalysis proceeding via a cysteine-phosphate intermediate. *J. Biol. Chem.* **266**, 17026-17030.

Gupton, S. L. and Waterman-Storer, C. M. (2006). Spatiotemporal feedback between actomyosin and focal-adhesion systems optimizes rapid cell migration. *Cell* **125**, 1361-1374.

Hagel, M., George, E. L., Kim, A., Tamimi, R., Opitz, S. L., Turner, C. E., Imamoto, A. and Thomas, S. M. (2002). The adaptor protein paxillin is essential for normal development in the mouse and is a critical transducer of fibronectin signaling. *Mol. Cell. Biol.* **22**, 901-915.

Haj, F. G., Verveer, P. J., Squire, A., Neel, B. G. and Bastiaens, P. I. (2002). Imaging sites of receptor dephosphorylation by PTP1B on the surface of the endoplasmic reticulum. *Science* **295**, 1708-1711.

Haj, F. G., Sabet, O., Kinkhabwala, A., Wimmer-Kleikamp, S., Roukos, V., Han, H. M., Grabenbauer, M., Bierbaum, M., Antony, C., Neel, B. G. and Bastiaens, P. I. (2012). Regulation of signaling at regions of cell-cell contact by endoplasmic reticulum-bound protein-tyrosine phosphatase 1B. *PLoS One* **7**, e36633.

Harms, B. D., Bassi, G. M., Horwitz, A. R. and Lauffenburger, D. A. (2005). Directional persistence of EGF-induced cell migration is associated with stabilization of lamellipodial protrusions. *Biophys. J.* **88**, 1479-1488.

Harte, M. T., Hildebrand, J. D., Burnham, M. R., Bouton, A. H. and Parsons, J. T. (1996). p130Cas, a substrate associated with v-Src and v-Crk, localizes to focal adhesions and binds to focal adhesion kinase. *J. Biol. Chem.* **271**, 13649-13655.

Hernández, M. V., Sala, M. G., Balsamo, J., Lilien, J. and Arregui, C. O. (2006). ER-bound PTP1B is targeted to newly forming cell-matrix adhesions. *J. Cell Sci.* **119**, 1233-1243.

Hernández, M. V., Wehrendt, D. P. and Arregui, C. O. (2010). The protein tyrosine phosphatase PTP1B is required for efficient delivery of N-cadherin to the cell surface. *Mol. Biol. Cell* **21**, 1387-1397.

Hirata, H., Tatsumi, H. and Sokabe, M. (2008). Mechanical forces facilitate actin polymerization at focal adhesions in a zyxin-dependent manner. *J. Cell Sci.* **121**, 2795-2804.

Honda, H., Oda, H., Nakamoto, T., Honda, Z., Sakai, R., Suzuki, T., Saito, T., Nakamura, K., Nakao, K., Ishikawa, T. et al. (1998). Cardiovascular anomaly, impaired actin bundling and resistance to Src-induced transformation in mice lacking p130Cas. *Nat. Genet.* **19**, 361-365.

Hu, C. D., Chinenov, Y. and Kerppola, T. K. (2002). Visualization of interactions among bZIP and Rel family proteins in living cells using bimolecular fluorescence complementation. *Mol. Cell* **9**, 789-798.

Itoh, R. E., Kurokawa, K., Ohba, Y., Yoshizaki, H., Mochizuki, N. and Matsuda, M. (2002). Activation of rac and cdc42 video imaged by fluorescent resonance energy transfer-based single-molecule probes in the membrane of living cells. *Mol. Cell. Biol.* **22**, 6582-6591.

Izaguirre, G., Aguirre, L., Hu, Y. P., Lee, H. Y., Schlaepfer, D. D., Aneskievich, B. J. and Haimovich, B. (2001). The cytoskeletal/non-muscle isoform of alpha-actinin is phosphorylated on its actin-binding domain by the focal adhesion kinase. *J. Biol. Chem.* **276**, 28676-28685.

Kaplan, K. B., Bibbins, K. B., Swedlow, J. R., Arnaud, M., Morgan, D. O. and Varmus, H. E. (1994). Association of the amino-terminal half of c-Src with focal adhesions alters their properties and is regulated by phosphorylation of tyrosine 527. *EMBO J.* **13**, 4745-4756.

Kaplan, K. B., Swedlow, J. R., Morgan, D. O. and Varmus, H. E. (1995). c-Src enhances the spreading of src-/- fibroblasts on fibronectin by a kinase-independent mechanism. *Genes Dev.* **9**, 1505-1517.

Klinghoffer, R. A., Sachsenmaier, C., Cooper, J. A. and Soriano, P. (1999). Src family kinases are required for integrin but not PDGFR signal transduction. *EMBO J.* **18**, 2459-2471.

Laukaitis, C. M., Webb, D. J., Donais, K. and Horwitz, A. F. (2001). Differential dynamics of α 5 integrin, paxillin, and α-actinin during formation and disassembly of adhesions in migrating cells. *J. Cell Biol.* **153**, 1427-1440.

Liang, F., Lee, S. Y., Liang, J., Lawrence, D. S. and Zhang, Z. Y. (2005). The role of protein-tyrosine phosphatase 1B in integrin signaling. *J. Biol. Chem.* **280**, 24857-24863.

Lim, Y., Lim, S. T., Tomar, A., Gardel, M., Bernard-Trifilo, J. A., Chen, X. L., Uryu, S. A., Canete-Soler, R., Zhai, J., Lin, H. et al. (2008). PyK2 and FAK connections to p190Rho guanine nucleotide exchange factor regulate RhoA activity, focal adhesion formation, and cell motility. *J. Cell Biol.* **180**, 187-203.

Lin, S. Y., Raval, S., Zhang, Z., Deverill, M., Siminovitch, K. A., Branch, D. R. and Haimovich, B. (2004). The protein-tyrosine phosphatase SHP-1 regulates the phosphorylation of alpha-actinin. *J. Biol. Chem.* **279**, 25755-25764.

Liu, F., Hill, D. E. and Chernoff, J. (1996). Direct binding of the proline-rich region of protein tyrosine phosphatase 1B to the Src homology 3 domain of p130(Cas). *J. Biol. Chem.* **271**, 31290-31295.

Martens, L., Monsieur, G., Ampe, C., Gevaert, K. and Vandekerckhove, J. (2006). Cell_motility: a cross-platform, open source application for the study of cell motion paths. *BMC Bioinformatics* **7**, 289-294.

Monteleone, M. C., González Wusener, A. E., Burdisso, J. E., Conde, C., Cáceres, A. and Arregui, C. O. (2012). ER-bound protein tyrosine phosphatase PTP1B interacts with Src at the plasma membrane/substrate interface. *PLoS One* **7**, e38948.

Nakamura, T., Aoki, K. and Matsuda, M. (2005). Monitoring spatio-temporal regulation of Ras and Rho GTPase with GFP-based FRET probes. *Methods* **37**, 146-153.

Nievergall, E., Janes, P. W., Stegmayer, C., Vail, M. E., Haj, F. G., Teng, S. W., Neel, B. G., Bastiaens, P. I. and Lackmann, M. (2010). PTP1B regulates Eph receptor function and trafficking. *J. Cell Biol.* **191**, 1189-1203.

Othmer, H. G., Dunbar, S. R. and Alt, W. (1988). Models of dispersal in biological systems. *J. Math. Biol.* **26**, 263-298.

Pathre, P., Arregui, C., Wampler, T., Kue, I., Leung, T. C., Lilien, J. and Balsamo, J. (2001). PTP1B regulates neurite extension mediated by cell-cell and cell-matrix adhesion molecules. *J. Neurosci. Res.* **63**, 143-150.

Pertz, O. (2010). Spatio-temporal Rho GTPase signaling - where are we now? *J. Cell Sci.* **123**, 1841-1850.

Rajfur, Z., Roy, P., Otey, C., Romer, L. and Jacobson, K. (2002). Dissecting the link between stress fibers and focal adhesions by CALI with EGFP fusion proteins. *Nature Cell Biol.* **4**, 286-293.

Ren, X. D., Kiosses, W. B. and Schwartz, M. A. (1999). Regulation of the small GTP-binding protein Rho by cell adhesion and the cytoskeleton. *EMBO J.* **18**, 578-585.

Richardson, A., Malik, R. K., Hildebrand, J. D. and Parsons, J. T. (1997). Inhibition of cell spreading by expression of the C-terminal domain of focal adhesion kinase (FAK) is rescued by coexpression of Src or catalytically inactive FAK: a role for paxillin tyrosine phosphorylation. *Mol. Cell. Biol.* **17**, 6906-6914.

Roskoski, R., Jr (2005). Structure and regulation of Kit protein-tyrosine kinase—the stem cell factor receptor. *Biochem. Biophys. Res. Commun.* **338**, 1307-1315.

Sakai, R., Nakamoto, T., Ozawa, K., Aizawa, S. and Hirai, H. (1997). Characterization of the kinase activity essential for tyrosine phosphorylation of p130Cas in fibroblasts. *Oncogene* **14**, 1419-1426.

Scales, T. M. and Parsons, M. (2011). Spatial and temporal regulation of integrin signalling during cell migration. *Curr. Opin. Cell Biol.* **23**, 562-568.

Schaller, M. D. and Parsons, J. T. (1995). pp125FAK-dependent tyrosine phosphorylation of paxillin creates a high-affinity binding site for Crk. *Mol. Cell. Biol.* **15**, 2635-2645.

Schaller, M. D., Hildebrand, J. D., Shannon, J. D., Fox, J. W., Vines, R. R. and Parsons, J. T. (1994). Autophosphorylation of the focal adhesion kinase, pp125FAK, directs SH2-dependent binding of pp60src. *Mol. Cell. Biol.* **14**, 1680-1688.

Schaller, M. D., Hildebrand, J. D. and Parsons, J. T. (1999). Complex formation with focal adhesion kinase: A mechanism to regulate activity and subcellular localization of Src kinases. *Mol. Biol. Cell* **10**, 3489-3505.

Schwartz, M. A. and Shattil, S. J. (2000). Signaling networks linking integrins and rho family GTPases. *Trends Biochem. Sci.* **25**, 388-391.

Tachibana, K., Urano, T., Fujita, H., Ohashi, Y., Kamiguchi, K., Iwata, S., Hirai, H. and Morimoto, C. (1997). Tyrosine phosphorylation of Crk-associated substrates by focal adhesion kinase. A putative mechanism for the integrin-mediated tyrosine phosphorylation of Crk-associated substrates. *J. Biol. Chem.* **272**, 29083-29090.

Takino, T., Tamura, M., Miyamori, H., Araki, M., Matsumoto, K., Sato, H. and Yamada, K. M. (2003). Tyrosine phosphorylation of the CrkII adaptor protein modulates cell migration. *J. Cell Sci.* **116**, 3145-3155.

Tilghman, R. W., Slack-Davis, J. K., Sergina, N., Martin, K. H., Iwanicki, M., Hershey, E. D., Beggs, H. E., Reichardt, L. F. and Parsons, J. T. (2005). Focal adhesion kinase is required for the spatial organization of the leading edge in migrating cells. *J. Cell Sci.* **118**, 2613-2623.

Tsien, R. Y. and Harootunian, A. T. (1990). Practical design criteria for a dynamic ratio imaging system. *Cell Calcium* **11**, 93-109.

Vicente-Manzanares, M., Choi, C. K. and Horwitz, A. R. (2009). Integrins in cell migration—the actin connection. *J. Cell Sci.* **122**, 199-206.

von Wichert, G., Haimovich, B., Feng, G. S. and Sheetz, M. P. (2003). Force-dependent integrin-cytoskeleton linkage formation requires downregulation of focal complex dynamics by Shp2. *EMBO J.* **22**, 5023-5035.

Webb, D. J., Donais, K., Whitmore, L. A., Thomas, S. M., Turner, C. E., Parsons, J. T. and Horwitz, A. F. (2004). FAK-Src signalling through paxillin, ERK and MLCK regulates adhesion disassembly. *Nat. Cell Biol.* **6**, 154-161.

Yoshigi, M., Hoffman, L. M., Jensen, C. C., Yost, H. J. and Beckerle, M. C. (2005). Mechanical force mobilizes zyxin from focal adhesions to actin filaments and regulates cytoskeletal reinforcement. *J. Cell Biol.* **171**, 209-215.

Yoshizaki, H., Ohba, Y., Kurokawa, K., Itoh, R. E., Nakamura, T., Mochizuki, N., Nagashima, K. and Matsuda, M. (2003). Activity of Rho-family GTPases during cell division as visualized with FRET-based probes. *J. Cell Biol.* **162**, 223-232.

Zaidel-Bar, R., Ballestrem, C., Kam, Z. and Geiger, B. (2003). Early molecular events in the assembly of matrix adhesions at the leading edge of migrating cells. *J. Cell Sci.* **116**, 4605-4613.

Zhang, Z., Lin, S. Y., Neel, B. G. and Haimovich, B. (2006). Phosphorylated alpha-actinin and protein-tyrosine phosphatase 1B coregulate the disassembly of the focal adhesion kinase x Src complex and promote cell migration. *J. Biol. Chem.* **281**, 1746-1754.

Zhang, X., Tee, Y. H., Heng, J. K., Zhu, Y., Hu, X., Margadant, F., Ballestrem, C., Bershadsky, A., Griffiths, G. and Yu, H. (2010). Kinectin-mediated endoplasmic reticulum dynamics supports focal adhesion growth in the cellular lamella. *J. Cell Sci.* **123**, 3901-3912.